We are IntechOpen, the world's leading publisher of Open Access books Built by scientists, for scientists

5,000
Open access books available

125,000
International authors and editors

140M
Downloads

Our authors are among the

154
Countries delivered to

TOP 1%
most cited scientists

12.2%
Contributors from top 500 universities

WEB OF SCIENCE™

Selection of our books indexed in the Book Citation Index in Web of Science™ Core Collection (BKCI)

Interested in publishing with us?
Contact book.department@intechopen.com

Numbers displayed above are based on latest data collected.
For more information visit www.intechopen.com

Chapter

Epileptic EEG Classification by Using Advanced Signal Decomposition Methods

Ozlem Karabiber Cura and Aydin Akan

Abstract

Electroencephalography (EEG) signals are frequently used for the detection of epileptic seizures. In this chapter, advanced signal analysis methods such as Empirical Mode Decomposition (EMD), Ensembe (EMD), Dynamic mode decomposition (DMD), and Synchrosqueezing Transform (SST) are utilized to classify epileptic EEG signals. EMD and its derivative, EEMD are recently developed methods used to decompose nonstationary and nonlinear signals such as EEG into a finite number of oscillations called intrinsic mode functions (IMFs). In this study multichannel EEG signals collected from epilepsy patients are decomposed into IMFs, and then essential IMFs are selected. Finally, time- and spectral-domain, and nonlinear features are extracted from selected IMFs and classified. DMD is a new matrix decomposition method proposed as an iterative solution to problems in fluid flow analysis. We present single-channel, and multi-channel EEG based DMD approaches for the analysis of epileptic EEG signals. As a third method, we use the SST representations of seizure and pre-seizure EEG data. Various features are calculated and classified by Support Vector Machine (SVM), k-Nearest Neighbor (kNN), Naive Bayes (NB), Logistic Regression (LR), Boosted Trees (BT), and Subspace kNN (S-kNN) to detect pre-seizure and seizure signals. Simulation results demonstrate that the proposed approaches achieve outstanding validation accuracy rates.

Keywords: epileptic EEG classification, empirical mode decomposition (EMD), dynamic mode decomposition (DMD), synchrosqueezing transform (SST), machine learning

1. Introduction

Epilepsy, affecting approximately 4 and 10 per 1000 people of the world's population, is one of the most common acute neurological diseases. EEG is the most frequently used technique for the diagnosis of epilepsy, prediction, detection, and classification of epileptic seizures owing to cost, safety, and easy applicability [1, 2]. In order to detect or monitor epilepsy patients, long-term electroencephalogram (EEG) signals, which are records of the electrical activity generated by the brain, should be inspected visually by expert neurologists. However, this examination method is very time-consuming, bothersome, not efficient, and subjective process. Therefore, utilizing signal processing, machine learning, and artificial intelligence

methods for automatic seizure prediction and detection from epileptic EEG signals has become an active research field [2–5].

In the literature, seizure prediction and detection studies have been carried out using successful signal processing approaches in which many spectral, temporal, nonlinear, and statistical properties are calculated.

Automatic seizure detection and prediction studies have been conducted based on time-domain features such as energy, mean value, skewness, and kurtosis values [6–8], exponential energy [6] and, and frequency domain features such as Power spectral density features [9].

Also, entropy-based features such as fuzzy entropy (FuzzyEn), and sample entropy (SampEn) [10], sigmoid entropy [11], approximate entropy (ApEn) [12], weighted Permutation Entropy (WPE) [13], have also been commonly utilized to detect and predict epileptic seizures.

Additionally, in several epileptic seizure detections and prediction study, nonlinear features such as cross-bispectrum [4], fractal dimension, detrended fluctuation analysis (DFA), Hurst's exponent [3, 12] have been utilized and promising results have been provided.

On the other hand, various Time-Frequency (FT) analysis approaches have been also performed for epileptic seizure distinguish. The wavelet transform and its derivative [5, 14], Discrete WT (DWT) and Wavelet Packed Decomposition (WPD) [7] based approaches were successfully utilized in the seizure classification studies. Another TF analysis approaches such as The Hilbert Vibration Decomposition (HVD) [15], Variational Mode Decomposition (VMD), Hilbert transforms (HT) [16], the smoothed pseudo-Wigner-Ville distribution (SPWVD) [17], Hilbert–Huang transform (HHT) [18], short-time Fourier transform (STFT) [14, 19], the analytic time-frequency flexible wavelet transform (ATFFWT) [20], The Wigner–Ville distribution (WVD) [21] have been frequently used in seizure detection and prediction studies.

EMD [7, 8, 22] and its derivative approaches such as bivariate empirical mode decomposition (BEMD) [23], multivariate empirical Mode Decomposition (MEMD) [24], ensemble Empirical Mode Decomposition (EEMD) [25] that decompose a given signal into a limited number of zero-mean oscillations called Intrinsic Mode Functions (IMFs) have been developed for the analysis of nonlinear and non-stationary signals and have been successfully used in many seizure detection or prediction studies.

Generally, traditional Fourier-based methods such as CWT or STFT are not very effective in the TF analysis of non-stationary biosignals like EEG [26–28]. Successful seizure classification studies have been carried out using the Synchrosqueezing Transform (SST) method [28], which has been developed based on CWT and STFT [26–29], in order to achieve better TF representations (TFRs) in recent years.

The dynamic mode decomposition (DMD) and derivative approaches, a new matrix decomposition method, that introduced as a solution to problems encountered in fluid flow analysis by Schmidt [30], has recently been used to analyze epileptic EEG signals [31, 32].

In this chapter, three different advanced signal analysis methods are utilized for the classification of seizure and seizure-free EEG signals. The pre-seizure and seizure EEG segments were investigated using *(i)* EMD and its derivative EEMD methods, *(ii)* DMD method, and finally, *(iii)* SST and traditional STFT methods to achieve high classification performances. The rest of this chapter is organized as follows. In Section 2, EEG data set used in this study and employed signal analysis methods are described. Computer simulation results and discussion on the results of three different approaches are presented in Section 3. Conclusions of the study are drawn in Section 4.

2. Classification of epileptic EEG signals

In this study, three different approaches are presented to distinguish seizure and seizure-free EEG segments. In the first method, various temporal, spectral, and non-linear features are extracted from the IMFs obtained using EMD and EEMD approaches. In the second method we present, epileptic EEG segments are analyzed using a simple matrix decomposition method, namely the DMD approach. Finally, in the third approach the SST method with high TF resolution is utilized to extract features and achieve high classification performance in distinguishing seizure and seizure-free EEG segments. The results of these three approaches are compared in line with the classification performances of various machine learning algorithms used in our study.

2.1 Data set (IKCU EEG data set)

In our study, EEG data recorded using the Neurofax EEG device from 16 different epilepsy patients (5 Female; 11 Male, the average age is 37.3∓7) in the Department of Neurology, Faculty of Medicine, İzmir Katip Celebi University are used. These EEG recordings are collected with a sampling frequency of 100 Hz using surface electrodes from 18 different EEG channels (Fp1-F7, F7-T1, T1-T3, T3-T5, T5-O1, Fp1-F3, F3-C3, C3-P3, P3-O1, Fp2-F8, F8-T2, T2-T4, T4-T6, T6-O2, Fp2-F4 F4-C4, C4-P4, P4-O2). It was informed by expert neurologists that the attacks in the used EEG data set are Frontal and Temporal lobes focused. Hence, 10 EEG channels (Fp1-F7, F7-T1, T1-T3, T3-T5, Fp1-F3, Fp2-F8, F8-T2, T2-T4, T4-T6, Fp2-F4) with a predominance of temporal and frontal lobes are used in our study. These EEG data are used in our study by obtaining the Ethical Approval of İzmir Katip Çelebi University Non-Invasive Clinical Research Ethics Committee dated 08.08.2019 and numbered 296.

2.2 Empirical mode decomposition and its variant

EMD approach in which signals decomposed into Intrinsic Mode Functions (IMF) with zero-mean oscillations, is the adaptive time-frequency analysis method for the non-linear and non-stationary processes. The sum of these obtained IMFs must be equal to the original signal [22, 24].

$$x[n] = \left(\sum_{l=1}^{L} IMF_l[n]\right) + R_L[n] \tag{1}$$

where $x[n]$ is the original analyzed signal, L denotes the number of IMFs and $R_L[n]$ indicates the residue.

Despite the successful results of the traditional EMD approach to analyze the non-stationary process, the problem named “mode mixing” is encountered where similar oscillations occur in different modes or different oscillations are observed in the same mode. In the EEMD method, by adding Gaussian white noise to the analyzed signal, the continuity of the signal in different frequency regions is ensured, and the mode mixing problem has been tried to be overcome. Then, the noisy signals obtained by adding white noises with different statistical properties were decomposed into IMFs by the EMD method. As a result of the EEMD method, the average IMFs value is obtained by taking the average of the IMFs group obtained as much as the number of white noise added [25].

$$x^i[n] = x[n] + g^i[n], \qquad i = 1, 2, \ldots, K. \tag{2}$$

Here, ensemble number is denoted by K value, $g^i[n]$ is indicates the added Gaussian noise at i^{th} iteration.

By using EMD approach, IMFs ($IMF^i_j[n], j = 1, \ldots, J^i$) of noisy signal $x^i[n]$ is obtained for the i^{th} iteration. IMFs are calculated for the EEMD approach by taking the average of the IMFs obtained after the number of ensembles (K) iterations.

$$\overline{IMF_j[n]} = \frac{1}{K}\sum_{i=1}^{K} IMF^i_j[n] \tag{3}$$

The first 3 IMFs obtained for an example pre-seizure and seizure EEG segments using EMD and EEMD methods are shown in **Figure 1**.

In our proposed EMD and EEMD based approach, IMFs of pre-seizure and seizure EEG segments are obtained. Following, the IMF selection process is performed using energy-based, correlation-based, power spectral density-distance based and statistical p-value based metrics, as described in [8]. Time (Energy, Mean value, Skewness, and Kurtosis values) [6, 7], spectral (Total power, Spectral Entropy, 1st, 2nd, and 3rd spectral moments) [9], and non-linear (Hurst Exponent and Higuchi Fractal Dimension) [3, 12] features are calculated using 3 highly voted

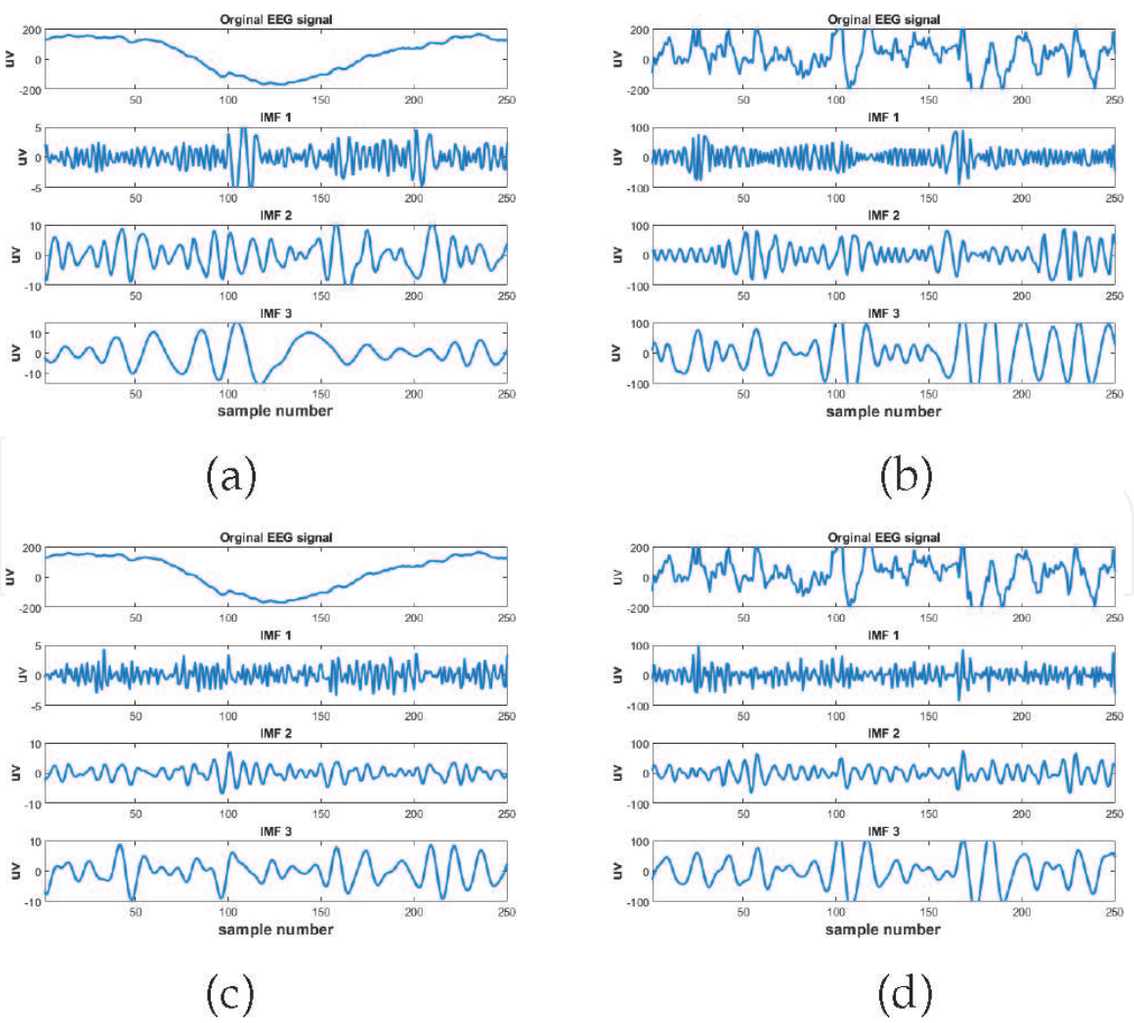

Figure 1.
Pre-seizure EEG signal and it's first three IMF obtained using (a) EMD, and (c) EEMD approaches; seizure EEG signal and it's first three IMF obtained using (b) EMD and (d) EEMD approaches.

IMFs (IMF1, IMF3, and IMF2) determined in the IMF selection process [8]. Thus, 4 time domain, 5 spectral, and 2 non-linear features are calculated for each pre-seizure and seizure EEG segment. For comparison, the same features are calculated from the EEG segment itself, without using the EMD or EEMD method. In addition, the same features are calculated from the sub-bands of the DWT approach, which is a conventional analysis method and compared with the results of the EMD and EEMD approach. In our experiments, Daubechies4 (db4) mother wavelet and 3 level subband decomposition are used [7, 33].

2.3 Dynamic mode decomposition

In fluid flow analysis studies, generally, computationally expensive Global stability analysis method where classical approaches are used, is performed. Proper Orthogonal Decomposition (POD) method based on snapshots of flow and achieving the most active modes is used in these methods. DMD approach based on matrix decomposition has been proffered as a solution to computationally cost of these previous approaches. Systems are analyzed in space using the DMD method in which temporal orthogonality is used. However, using the POD method utilizing spatial orthogonality, systems could be analyzed in time [30]. The behavior of non-linear and dynamic systems such as biological signals cannot be completely revealed by classical time-frequency analysis methods. By evaluating the measurements collected over a certain period of time with the DMD method, both the system can be expressed with a function, and information about the future behavior of the system can be predicted. The basic idea of the DMD method is to obtain the dynamic modes that best represent the system by achieving the eigenvalues and eigenvectors of the system that linearized with the Least-Squares Approximation (LSA) method [31, 34].

In literature, previously, $K \times T-$ sized multi-channel EEG signals are evaluated using the DMD approach. Here, T is the sample size of a single EEG channel, and N is the number of channels. Using this data matrix, $K \times L-$ sized X data matrices in which L denotes the time samples named "snapshot" is obtained, and the DMD algorithm is applied to this obtained data matrices [31]. In our study, both the multi-channel DMD approach used in the literature is performed and the single-channel DMD approach is proposed, unlike the literature, and $K \times L-$ sized X data matrices are constructed using this two different approaches.

In the **single-channel DMD approach (SC-DMD)**, the single-channel EEG signals with $T-$ samples long are divided into non-overlapping, L samples long EEG segments. The $(K \times L)$ EEG data matrices are constructed using K of these obtained segments. For our epileptic seizure classification experiment, $L = 140$ and $K = 5$ are chosen.

Additionally, in the **multi-channel DMD approach (MC-DMD)**, $(K \times L)$ EEG data matrices with no overlap are generated using $L = 140$ samples of $K = 5$ different EEG channels. In our experiment, these data matrices are obtained using the $K = 5-$EEG channel in the left hemisphere (Fp1-F7, F7-T1, T1-T3, T3-T5, Fp1-F3) and the $K = 5-$EEG channel in the right hemisphere (Fp2-F8, F8-T2, T2-T4, T4-T6, Fp2-F4). Also (10×120) EEG data matrices are constructed using the $K = 10-$EEG channel with $L = 120$ sample long in both hemispheres.

In order to achieve a sufficient number of modes to demonstrate the dynamics of neurological activity efficiently, the number of (K) measurements must be at least twice the number of L time points named snapshots [16]. Therefore, the data augmentation process is applied to the data matrix X based on the Hankel matrix creation principle as detailed in [34] and the $N \times M$, $(N \geq 2M)$ dimensional augmented data matrix X_a is obtained.

$$X_a = \begin{bmatrix} \vdots & \vdots & \dots & \vdots \\ x_1 & x_2 & \dots & x_{M-1} \\ \vdots & \vdots & \dots & \vdots \end{bmatrix} \qquad X'_a = \begin{bmatrix} \vdots & \vdots & \dots & \vdots \\ x_2 & x_3 & \dots & x_M \\ \vdots & \vdots & \dots & \vdots \end{bmatrix} \tag{4}$$

$$X'_a = AX_a \tag{5}$$

Transition matrix A that denoted in Eq. (5) should be obtained to achieve relation based on the high-dimensional linear regression between Xa matrix and its time-shifted version X'_a matrix (given in Eq. (4)). This transition matrix can be calculated using the pseudo-inverse of the X_a matrix $\left(A = X'_a X_a^+\right)$, but for higher-dimensional data such as biosignal, this can cause computational complexity. Using the DMD algorithm;

Singular value decomposition (SVD) of augmented data matrix $X_a = U\Sigma V^*$ is calculated, and formulation of transition matrix rewrite again using the Left singular vectors U, the inverse of the singular values Σ^{-1}, and the Right singular vectors V $A = X'_a X_a^+ = X'_a V\Sigma^{-1}U^*$. The low-rank approximation value $\tilde{A}$ of the transition matrix A can be obtained using Eq. (6)

$$\tilde{A} = U^* X'_a V\Sigma^{-1} \tag{6}$$

The Eigen decomposition of $\tilde{A}$ matrix is calculated ($\tilde{A}W = W\Omega$) and the matrix of eigenvectors W, the diagonal matrix Ω of eigenvalues are achieved. Finally, DMD modes of augmented data matrix X_a are calculated using Eq. (7) where each column of ϕ includes the DMD mode ϕ_m related to eigenvalues λ_m [31, 34].

$$\phi = X'_a V\Sigma^{-1}W \tag{7}$$

In our DMD based epileptic seizure classification experiment, using the DMD spectrum, various features based on DMD subband powers and Higher-order DMD spectral moments (DMD-HOS) are calculated and classification performances of approaches are compared.

The real part, of DMD modes associated with the complex eigenvalues λ_m, indicates the decay frequency of the dynamic modes, while the imaginary part of these modes shows the oscillation frequencies of the dynamic modes. To obtain the DMD spectrum of pre-seizure and seizure EEG segments, oscillation frequencies, and powers, of the dynamic modes, should be calculated. The oscillation frequencies f_m (Hz) are calculated using $\Delta t = 0.01s$ time difference between sequential snapshots, and the complex eigenvalues λ_m of DMD modes; $f_m = |imag\left(\frac{\omega_m}{2\pi}\right)|$, $\omega_m = \frac{log\,(\lambda_m)}{\Delta t}$ (the imaginary part of a complex number is calculated using $imag(.)$ operation). The frequency set $F_{DMD} = \{ f_m \}$ is obtained by aligning the oscillation frequencies containing different mode frequencies. Additionally, power $P_m = \|\phi_m\|^2$ of these modes are calculated using the Euclidian norm [34]. The total DMD mode power $\{ f_m \} \in F_{DMD}$ (given in Eq. (8)) for the f_m frequency is calculated by summing the power value of L_k DMD modes at the f_m frequency. This process is repeated for all frequencies in the F_{DMD} set and a single DMD power corresponding to each frequency is calculated. In order to obtain the **DMD spectrum**, the obtained DMD power set P_{DMD}, $\forall\{P_{DMD}(f_m)\} \in P_{DMD}$ is plotted according to the oscillation frequency set F_{DMD}.

$$P_{DMD}(f_m) = \sum_{i=1}^{L_k} P_m^i(f_m) \qquad \forall\{f_m\} \in F_{DMD}. \tag{8}$$

To reveal the advantages of the DMD approach, the traditional Power Spectral Density is estimated using the Welch method [5, 35] where the Hamming window and 50% overlapping are chosen, for each seizure, and pre-seizure EEG segments (140 samples long = 1.4 sec). Examples of the proposed Single-Channel EEG based DMD spectra and traditional Welch PSD estimates for pre-seizure and seizure epileptic EEG data are demonstrated in **Figure 2**. The similarity between the average PSD values of the 5 EEG segments (shown with bold black lines in **Figure 2(c)** and **(f)**) whose PSDs are calculated separately by the Welch method and the DMD spectrum, given in **Figure 2(b)** and **(e)**, is remarkable.

In DMD based epileptic seizure detection approach, sub-band powers based and DMD-HOS moments based features are introduced using the DMD spectrum. In computer-aided epileptic seizure detection and prediction studies, EEG subband powers of different frequency bands like delta (0–4 Hz), theta (4–8 Hz), alpha (8–12 Hz), beta (12–30 Hz), and gamma (30–60 Hz), and DMD-HOS moments are calculated using conventional Power Spectral Density [17, 40]. Using the estimated DMD spectrum, similar to the classical PSD approach, Delta (P_δ), Theta (P_θ), Alpha (P_α), Beta (P_β), and Gamma (P_γ)) **subband powers** are calculated as

$$P_{sb} = \sum_{f_m \in f_{sb}} P_{DMD}(f_m), \quad sb = \{\delta, \theta, \alpha, \beta, \gamma\} \qquad P_T = \sum_{f_m} P_{DMD}(f_m) \tag{9}$$

We propose another set of features called **DMD-HOS moments** $M^j_{DMD}, j = 1, 2, 3, \cdots$ defined by

$$M^j_{DMD} = \sum_{f_m \in F_{DMD}} (f_m)^j P_{DMD}(f_m), \qquad j = 1, 2, 3, \cdots \tag{10}$$

In Eqs. (9) and (10), f_{sb} is a subset of oscillation frequencies in $F_{DMD} = \{f_m\}$ of extracted DMD modes corresponding to sub-band frequencies $\{f_\delta, f_\theta, f_\alpha, f_\beta, f_\gamma\}$

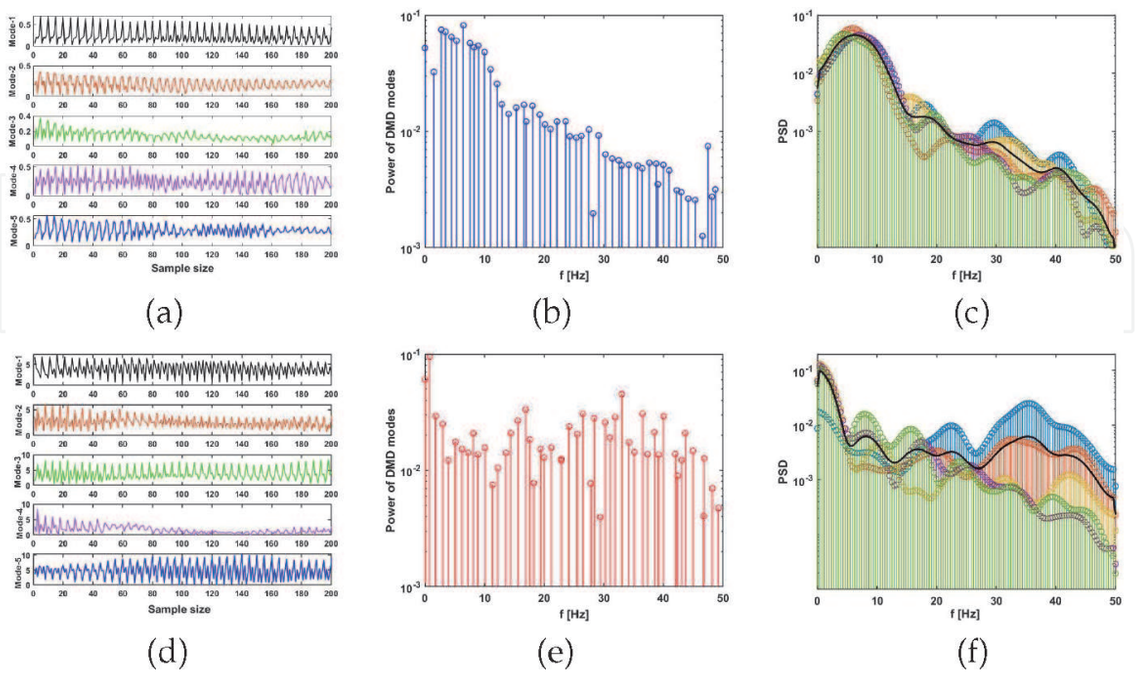

Figure 2.
First 5 DMD modes of 5 pre-seizure EEG segments (a) and its DMD spectrum (b) obtained using Single Channel EEG based dynamic mode decomposition, PSD of these 5 pre-seizure EEG segments together (c); first 5 DMD modes of 5 seizure EEG segments (d) and its DMD spectrum (e) obtained using Single Channel EEG based dynamic mode decomposition, PSD of these 5 seizure EEG segments together (f). Bold black lines denote the average of 5 PSD in (c) and (f).

of EEG, P_T denotes the total power of DMD spectrum, and M_{DMD}^{j} indicates the j^{th} order DMD spectral moment. In our computations, we extract 6 DMD subband power-based features, and 3 DMD-HOS moments features for each seizure and pre-seizure EEG segment.

2.4 Synchrosqueezing transform

Synchrosqueezing Transform is a member of TF reassignment methods (RM) family which developed to improve the localization properties of TFRs. In RM methods, using the reassignment process, TF coefficients $X(t,\omega)$ that computed utilizing classical TF analysis method, are reassigned into the instantaneous frequency (IF) trajectory close to the ideal TFR which have high frequency and time resolution $(t,\omega) \mapsto (\tau_0(t,\omega), \omega_0(t,\omega))$. On the other hand, using the squeezing process, this TF coefficients $X(t,\omega)$ are squeezed into the IF trajectory close to the ideal TFR which have high-resolution in only frequency $(t,\omega) \mapsto (t, \omega_0(t,\omega))$. Although lower TF resolution is achieved using the SST method, signal reconstruction may be performed [29, 36].

SST method based on STFT or CWT can be performed to obtain high-resolution TFRs of signals. Hence, the TF coefficients of the studied signals are obtained by STFT or CWT, and by using these coefficients with the SST approach, high-resolution TFR is obtained.

In the STFT method, the signal is divided into short-time, and usually overlapping segments and the Fourier transforms of these short-term segments are calculated. In our computations, STFT of 1-second EEG segment $x(t)$, are calculated as, $X(t,\omega) = \int_{-\infty}^{\infty} x(\tau) w(\tau - t) e^{-j\omega\tau} d\tau$ where $w(t)$ denotes the used window function. Using the Fourier transforms of analyzed segment $X(\omega)$ and used window function $W(\omega)$, STFT may be rewritten again as given in Eq. (11).

$$X(t,\omega) = \frac{1}{2\pi} \int_{-\infty}^{\infty} X(\xi) W(\omega - \xi) e^{j\xi t} d\xi. \tag{11}$$

In the SST approach, computing the derivative of STFT $X(t,\omega)$ according to time, the instantaneous frequency $\omega_0(t,\omega) = -j \frac{\partial_t X(t,\omega)}{X(t,\omega)}$ is obtained. By using synchrosqueezing operator $\int_{-\infty}^{\infty} \delta(\eta - \omega_0(t-\omega)) d\omega$ of SST and IF ω_0(t, ω), SST $T(t,\eta)$ with high-resolution is obtained by collecting the STFT coefficients which have the same frequency where they should appear.

$$T(t,\eta) = \int_{-\infty}^{\infty} X(t,\omega) \delta(\eta - \omega_0(t-\omega)) d\omega \tag{12}$$

An example TF representations of 1-sec pre-seizure and seizure EEG segments achieved utilizing SST and STFT approaches are shown in **Figure 3**. We observe in **Figures 3(b)**, **(c)**, **(e)** and **(f)** that the SST approach is able to represent pre-seizure and seizure EEG segments better in the TF plane than the STFT method. Although the window size, which is the most important parameter of STFT [19], is chosen to give the best time and frequency resolution, the SST approach provided better TF resolution.

In our SST based epileptic seizure detection study, high-resolution joint TF distributions of pre-seizure and seizure EEG segments are calculated. Two different feature extraction approaches are presented to achieve efficient features from the magnitude square of the SST matrix $S(n,\omega_k)$:

a. Log-normalized **higher-order joint TF (HOJ-TF) moments**, $\overline{<n^i\ \omega_k^j>}; i,j = 1, 2, \ldots$ [37],

$$\overline{<n^i\ \omega_k^j>} = \log\left(\frac{\sum_{n=0}^{N-1}\sum_{k=0}^{N-1} n^i \omega_k^j S(n,\omega_k)}{i!j!}\right), \qquad i,j = 1, \ldots \tag{13}$$

where N is the length of the EEG segments, and $\omega_k = \frac{2\pi}{N}k, k = 0, \ldots, N-1$.

b. TFR obtained by SST is used as image and **Gray Level Co-occurrence Matrix (GLCM)** texture descriptors are obtained from this TFR image.

GLCM is a prediction of the joint probability distribution of two neighboring gray-level image pixel pairs with a certain position that consists of distance (d) and direction (θ) information. The GLCM of this image can be expressed as given in Eq. (14) using image pixel pair position information ($\Delta = (\theta, d)$).

$$G_\Delta(i,j) \qquad (i,j = 0,1, \ldots, N_g - 1) \tag{14}$$

where, i and j indicate the intensity values of two pixels, and N_g is the number of gray levels in the image [28, 38]. Second-order statistical features such as contrast, correlation, energy, and homogeneity [39] are calculated as features from the GLCM matrix of TF images corresponding to pre-seizure and seizure EEG segments. In order to evaluate the performance of the SST approach, same features are calculated using the magnitude square of STFT, i.e., the spectrogram $|X(t,\omega)|^2$, which is a classical TF approach and is also used in the SST algorithm [19]. In our experiments, 3 HOJ-TF moments based features, and 4 GLCM based features are calculated for each pre-seizure and seizure EEG segment using both SST and STFT approaches.

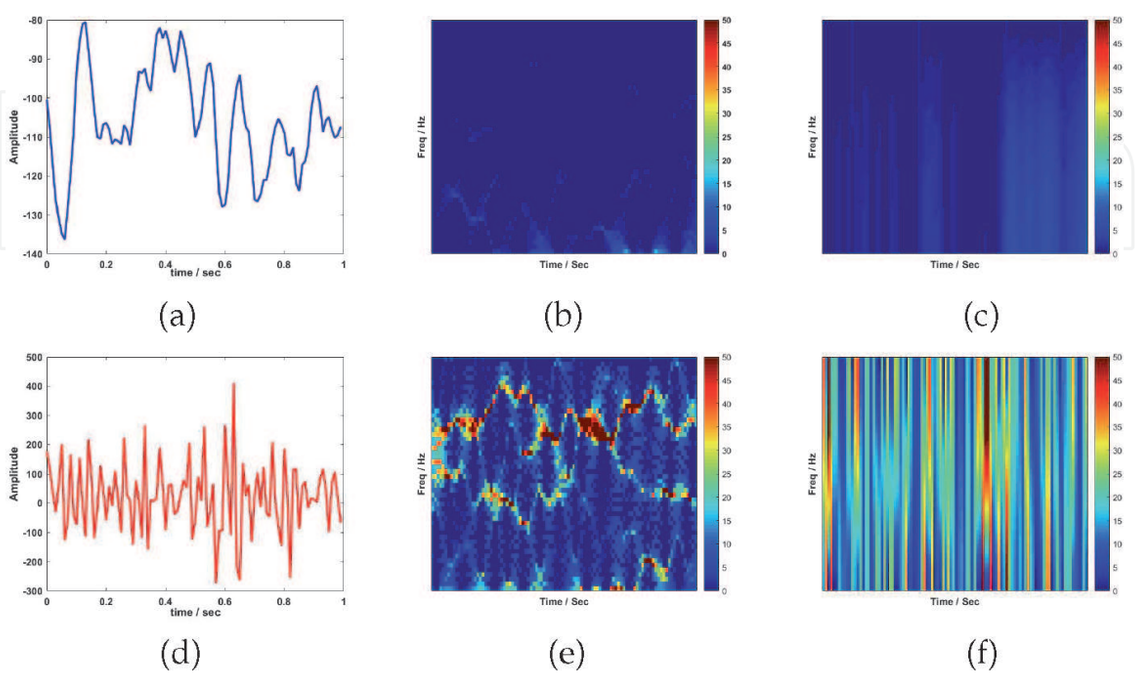

Figure 3.
(a) 1-sec pre-seizure EEG segment, its (b) magnitude SST, and (c) magnitude STFT; (d) 1-sec seizure EEG segment, its (e) magnitude SST, and (f) magnitude STFT.

2.4.1. Classification and performance evaluation

In the proposed study, features extracted utilizing the three different approaches are classified using six different classifiers such as SVM, kNN, NB to distinguish seizure and pre-seizure EEG segments.

In SVM, one of the well-known supervised learning algorithms, decision boundaries, called hyper-planes', is determined to categorize data. While there are many possible hyper-planes that may be constructed, it is essential to determine the hyper-plane where the best classification performance is obtained. The optimal hyper-plane is achieved by maximizing the margin, which is the distance between different classes' support vectors. Once the optimum hyper-plane is determined, the data falling on different sides of the hyper-plane are assigned as elements of different classes. While this process used for the only linearly separable datasets, using the kernel functions SVM is performed to distinguish linearly non-separable datasets. In our proposed study, linear kernel function is performed [10, 13].

The basic and efficient machine learning method kNN is one of the most widely used supervised learning approaches. The distance between each sample x_0 to be classified in the test data and the training data is calculated for all data set which is randomly divided into tests and trains. By determining the k neighbors that have the minimum distance, the most common class among these k neighbors is assigned as the class of this sample. Although there are various distance calculation metrics such as Euclidean, Manhattan, Minkowski, and Hamming, the Euclidean distance metric, which is the most commonly used in the literature, is used in our study. In addition, the value of k is chosen as 10 for the proposed study [39, 40].

The NB classifier is one of the probabilistic classifiers in which the classification is performed according to Bayes' theorem. Membership probabilities $P(M_i/x_0)$ (M_i indicates the class, c denotes the number of class) to "c" classes of sample x_0 to be classified are calculated, separately. This sample is assigned as a member of the class in which the highest probability of membership among the "c" class is calculated [39, 40].

To achieve a stable classification accuracy, 10–fold cross-validation is employed in our experiment. Using Accuracy (ACC), and $F1$-score metrics, performance evaluation of proposed methods and utilized classifiers are investigated.

$$ACC = \frac{TP + TN}{TP + FN + FP + TN}, \quad F_{Score} = 2 * \frac{PRE * REC}{PRE + REC} \tag{15}$$

where true-positive (TP) is the number of samples of *class*_1 classified in the same class, and true-negative (TN) denotes the number of samples of *class*_0 classified in *class*_0. While false-positive (FP) is the number of samples not in *class*_1 but classified in *class*_1, false-negative (FN) indicates the number of samples in *class*_1 but classified in *class*_0. Recall and Precision metrics are formulated respectively as, $REC = \frac{TP}{TP+FN}$, and $PRE = \frac{TN}{FP+TN}$ [18].

3. Experiments and results

In the following, we give the performance evaluation of seizure and pre-seizure EEG classification by using three different advanced signal representation methods presented in Section 2. The classification process is performed using SVM, kNN, and NB classifiers and compared the performance of each approach and classifier. In the **Tables 1**-5, highest classification performances are indicated with boldface numbers for each approach and component.

		SVM		kNN		NB	
Approach	**Components**	**ACC**	**F-Score**	**ACC**	**F-Score**	**ACC**	**F-Score**
EMD	IMF1	94.31	94.16	94.38	94.31	94.31	94.03
	IMF2	94.12	93.85	92.62	92.48	93.13	92.79
	IMF3	93.38	93.36	94.63	94.45	95.63	95.48
	IMF1-IMF2	**94.56**	**94.40**	93.81	93.70	94.56	94.33
	IMF1-IMF3	92.06	92.38	**95.63**	**95.53**	**96.88**	**96.77**
	IMF2-IMF3	94.50	94.35	94.81	94.66	95.88	95.74
	IMF1-3	90	90.99	94.88	94.81	96.19	96.07
EEMD	IMF1	**96.06**	**96.04**	94.44	94.43	93.75	93.60
	IMF2	92.44	92.19	91.81	91.69	93.50	93.12
	IMF3	94.50	94.42	94.06	94.02	95.44	95.27
	IMF1-IMF2	94.94	94.86	94.81	94.76	94.12	93.91
	IMF1-IMF3	81.69	80.29	95.94	95.90	**97**	**96.91**
	IMF2-IMF3	94.44	94.32	94.25	94.21	95.38	95.18
	IMF1-3	94.19	94.39	**97**	**96.97**	95.75	95.62
DWT	AC + DC1-3	80.81	76.83	93.44	93.38	**94.56**	**94.43**
EEG	all EEG	59.75	66.33	**93.25**	**93.35**	78.94	74.41

Table 1.
Performance results (%) of EMD and EEMD based seizure detection approach.

		SVM		kNN		NB	
Approach	**Components**	**ACC**	**F-Score**	**ACC**	**F-Score**	**ACC**	**F-Score**
SC-DMD	Right Hems.	90.3	91.9	90.8	92.9	89.4	91.2
	Left Hems.	93.7	95.1	**94.1**	**95.5**	93.4	94.6
	Two Hems.	91.7	93.4	92.3	93.9	91.3	92.8
MC-DMD	Right Hems.	90.6	91.9	89.3	90.9	89.5	91.7
	Left Hems.	92.9	94.8	**93.9**	**95.5**	92.7	93.8
	Two Hems.	94.7	95.9	94.5	95.9	93.5	94.4
PSD	Right Hems.	86.1	88.7	87.2	89.9	86.7	86.2
	Left Hems.	92.1	93.4	**92.2**	**93.9**	91.3	93.4
	Two Hems.	89.1	91.3	89.5	91.5	88.3	90.7

Table 2.
Performance results (%) for seizure detection using the subband power based feature set of DMD based approach.

3.1 Results of EMD methods

In EMD and EEMD based seizure detection approaches, various features in the time-domain, spectral-domain, and non-linear are calculated to separate the seizure and pre-seizure EEG segments. To compare the performances of EMD based approaches, DWT approach is implemented to the pre-seizure and seizure EEG

		SVM		kNN		NB	
Approach	**Components**	**ACC**	**F-Score**	**ACC**	**F-Score**	**ACC**	**F-Score**
SC-DMD	Right Hems.	87.3	89.4	88.4	90.5	83.1	85.8
	Left Hems.	**92.2**	**93.9**	91.2	93.9	90.1	92.9
	Two Hems.	89.7	92.4	90.2	92.5	87	89.3
MC-DMD	Right Hems.	88.9	90.9	85.9	89.4	81.2	84.4
	Left Hems.	**92.9**	**93.4**	92	93.9	87.6	89.7
	Two Hems.	92.8	94.4	92.2	93.5	88.8	90.4
PSD	Right Hems.	85.6	87.6	88.1	90.9	86.8	88.2
	Left Hems.	**92.5**	**93.9**	91.6	93.5	92.5	93.9
	Two Hems.	88.6	90.3	89.4	91.5	89.2	91.3

Table 3.
Performance results (%) for seizure detection using the DMD-HOS moment based feature set of DMD based approach.

		SVM		kNN		NB	
Approach	**Components**	**ACC**	**F-Score**	**ACC**	**F-Score**	**ACC**	**F-Score**
SST	Right Hems.	88.4	91.1	**88.5**	**91.1**	83.6	86.2
	Left Hems.	**93.1**	**94.6**	92.5	94.2	92.1	93.7
	Two Hems.	**90.5**	**92.6**	90.1	92.3	88	90.2
STFT	Right Hems.	**87.2**	**90.1**	86.6	89.5	79.1	81.7
	Left Hems.	**92.1**	**93.8**	91.6	93.5	85.3	87.7
	Two Hems.	**89.5**	**91.7**	89.1	91.4	82.2	84.8

Table 4.
Performance results (%) for seizure detection using the HOJ-TF moment based feature set of SST and STFT based approaches.

		SVM		kNN		NB	
Approach	**Components**	**ACC**	**F-Score**	**ACC**	**F-Score**	**ACC**	**F-Score**
SST	Right Hems.	**88.6**	**91.2**	88.4	91	88.1	90.6
	Left Hems.	92.5	94.1	**92.6**	**94.2**	92.2	93.9
	Two Hems.	**90.4**	**92.4**	90	92.2	90.1	92.2
STFT	Right Hems.	**85.4**	**88.6**	85	88.2	83.8	87.3
	Left Hems.	90.3	92.4	**90.4**	**92.4**	88.7	91.1
	Two Hems.	**87.5**	**90.2**	87.4	90	86.2	89.1

Table 5.
Performance results (%) for seizure detection using the GLCM based feature set of SST and STFT based approaches.

segments, and same features are calculated from the Approximation Coefficient (AC) and 3 Detail Coefficients (DC) of DWT. Additionally, without using any signal processing approach the same features are extracted from the EEG signals itself.

The performance evaluation results for different IMF combinations are demonstrated in **Table 1**. In all tables, we indicate the highest classification performance with boldface numbers for each case. In **Table 1**, the components column shows that the features for classifications are calculated by using the corresponding component. For example, the classification results of the features calculated using IMF1 are given in the first row, and the classification results of the features calculated from the EEG signal itself are given in the last row. NB classifier provides the highest classification successes for both EMD (96.88% ACC, 96.77% *F*1-score) and EEMD (97% ACC, 96.91% *F*1-score) approaches by using features calculated from IMF1-IMF3 (the first two IMFs decided by the IMF selection process) of the corresponding approach. While, the maximum (94.56% ACC, 94.43% *F*1-score) classification successes are achieved using the NB classifier for the DWT approach; using the kNN classifier and EEG signals itself, maximum (93.25% ACC, 93.35% *F*1-score) values are obtained.

3.2 Results of DMD methods

Performance evaluation results of SC-DMD and MC-DMD based and PSD based epileptic seizure detection approaches are summarized in **Tables 2**-**3**. For the SC-DMD and PSD approaches, the classification results of the feature set created by combining the features obtained from the Left Hemisphere (Fp1-F7, F7-T1, T1-T3, T3-T5, Fp1-F3), Right hemisphere (Fp2-F8, F8-T2, T2-T4, T4-T6, Fp2-F4), and both hemisphere (Fp1-F7, F7-T1, T1-T3, T3-T5, Fp1-F3, Fp2-F8, F8-T2, T2-T4, T4-T6, Fp2-F4) channels separately are denoted with "Left Hems", "Right Hems "and "Two Hems", while the same components show the classification results of DMD features obtained from the EEG data matrix created using the respective hemisphere channels in the MC-DMD approach.

For all three approaches, the highest classification performance for both the subband based feature set and the moment based feature set is obtained from the Left Hems. While the kNN classifier is yield to highest classification accuracy 94.1% and *F*1-score 95.5% for subband power-based feature set obtained from the Left Hems of SC-DMD approach, the maximum 92.2% ACC and 93.9% *F*1-score values are achieved with the SVM classifier using the moment-based feature set of the SC-DMD approach. On the other hand, in the MC-DMD approach, the classification performances of subband power-based (kNN: 93.9% ACC, 95.5% *F*1-score) and moment-based (SVM: 92.9% ACC, 93.4% *F*1-score) feature sets are close to each other for Left Hems and Two Hems. Additionally, using the PSD approach, a maximum of 92.2%, and 92.5% classification accuracies are achieved using the kNN and SVM classifiers for the subband power-based and moment-based feature sets of Left Hems, respectively. The results show that both SC-DMD and MC-DMD approaches are more successful than the classical PSD approach.

3.3 Results of SST and STFT methods

Performance evaluation results of the SST based approach are given in **Tables 4**, **5**. Analyzes for SST and STFT approaches are carried out separately for each channel. The classification result of the feature set created by combining the features obtained from the left hemisphere channels is given with the "Left Hems" component. Similarly, while the classification result of the feature set obtained for the right hemisphere is given with "Right Hems", the classification result of the feature set created by combining the features obtained from all channels is given with the "Two Hems" component.

Classification performance of HOJ-TF based feature set is higher than that of GLCM based feature set for each component of SST and STFT approaches. In both

approaches, the classification success of both the HOJ-TF moment based feature set and the GLCM based feature set is higher in Left Hems than in Right Hems. While the highest 93.1% ACC and 94.6% *F*1-score are provided with SVM classifier by using the HOJ-TF moment-based feature set for Left Hems of SST, the maximum 92.6% ACC and 94.2% *F*1-score are obtained with the kNN classifier using the GLCM based feature set. On the other hand, in the STFT approach, 92.1% ACC and 93.8% *F*1-score values are achieved with the SVM using the HOJ-TF moment-based feature set, while the classification performance of GLCM based feature set is 90.4% ACC, and 92.4% *F*1-score for kNN classifier.

*F*1-scores obtained by the proposed methods, and by the classical approaches are calculated for comparison and given in **Figure 4**. The *F*1-scores of the proposed EMD and EEMD-based approaches, in **Figure 4a**, are higher than those of DWT and EEG-based approaches, except for the kNN classifier. In the DMD-based seizure detection approach, higher *F*1-score values are obtained in all classifiers than that of the traditional PSD approach for the subband power-based feature set, while the DMD approach provided higher *F*1-score values in the moment-based feature set, except for the NB classifier, shown in **Figure 4b**. Finally, in the SST-based epileptic seizure detection approach, higher *F*1-score values are obtained for each feature set and classifier compared to the STFT approach as shown in **Figure 4c**.

Channel-based classification performances of the proposed SC-DMD, SST, EMD, and EEMD approaches are given with a topographic maps in **Figure 5**. The topographic map is created by averaging the ACC values obtained with all classifiers for each method. It was stated by the expert neurologists that epileptic attacks in the used data set are left hemisphere-focused. It is noteworthy that the channel-based classification success of the EEG-based seizure detection approach (shown in **Figure 5a**) is very low, while is very high for the EEMD-based seizure detection approach (given in **Figure 5c**). It is also remarkable that in all proposed methods, the channels in the left hemisphere yielded successful results of seizure detection (given in **Figure 5b**-**5e**).

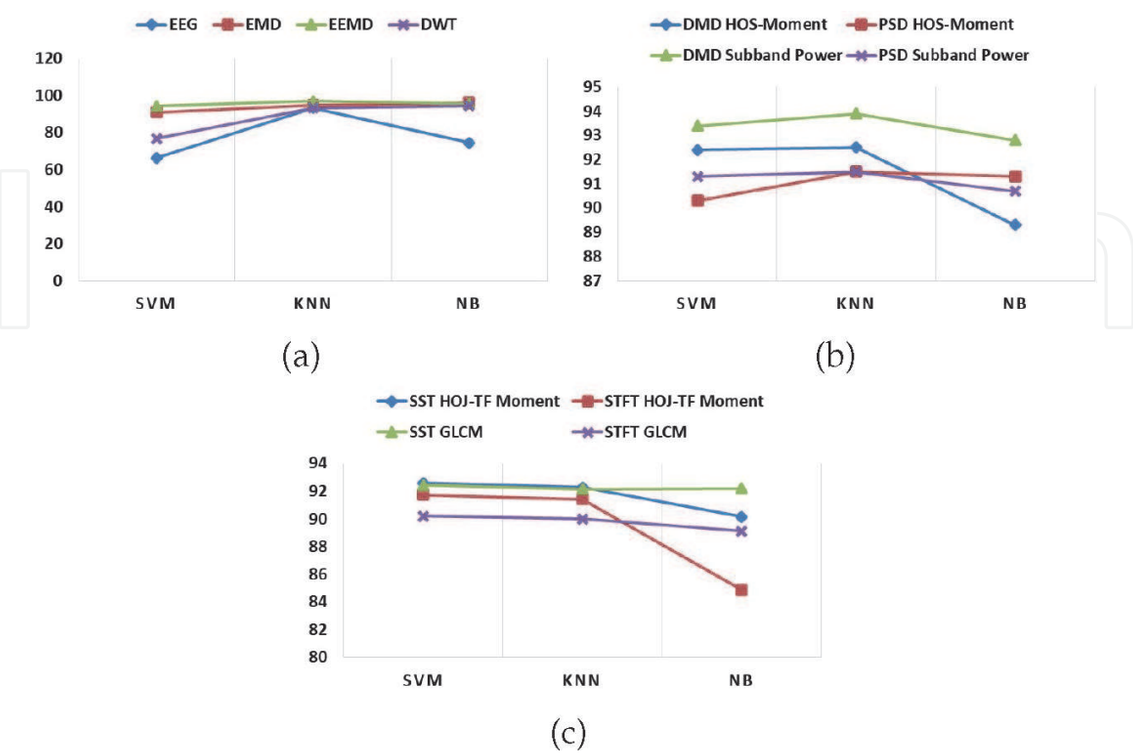

Figure 4.
Changing of F1-score values of (a) EMD and EEMD based, (b) DMD based, and (c) SST and STFT based epileptic seizure detection approaches.

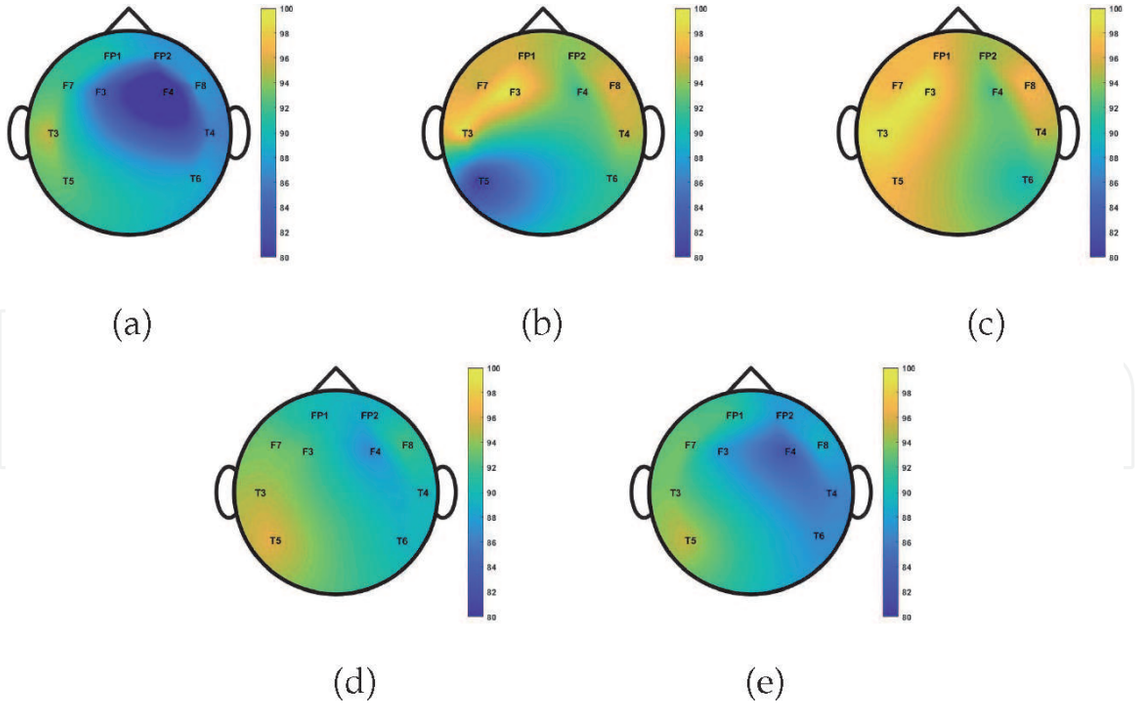

Figure 5.
Topographic map of channel based classification accuracies of (a) EEG based (b) EMD based (c) EEMD based (d) SC-DMD based, and (e) SST based approaches.

4. Conclusions

In our study, epileptic seizure detection is performed using EMD and derivative approaches, the DMD approach, which is a matrix decomposition method, and the SST approach, a new TF method. Pre-seizure and seizure EEG segments are decomposed into IMFs using the EMD and EEMD method, and time, spectral and non-linear features are calculated using the first 3 IMFs (IMF1, IMF3, IMF2) after the IMF selection process which detailed in our previous study [18]. In order to compare the success of EMD and EEMD methods, the same features are obtained using the approximation and detail coefficient of the DWT approach and directly from the EEG signal itself. While the EEMD method gives more successful results than the EMD approach for all conditions and classifiers, the most unsuccessful classification results are obtained by using features calculated from the EEG signal itself.

DMD spectra are obtained for pre-seizure and seizure EEG segments using the DMD approach, which is a simple matrix decomposition method. Although the DMD spectrum has been defined in the literature [31, 34], different features other than DMD powers have not been calculated using this spectrum. In our study, it is proposed to calculate DMD subband powers and DMD-HOS moments as features. In addition, although the multi-channel DMD approach has been used in the literature, the single-channel DMD approach has been proposed in our study. The success of the DMD approach is compared with the classical PSD obtained using the Welch method. The classification performance of both MC-DMD and SC-DMD approaches is higher than that of the PSD approach. In addition, the proposed SC-DMD based approach has been at least as successful as the MC-DMD based approach.

Another seizure detection study is carried out using the high TF resolution SST approach which proposed to overcome the disadvantages of classical TF approaches. HOJ-TF moment-based and GLCM-based features are calculated as features using the magnitude square of SST. The same features are computed using

the STFT method that is the classical TF analysis method to compare the success of SST. The SST approach provided higher classification accuracy than STFT for each condition and classifier.

EMD and EEMD approaches with high computational complexity [18], yielded more successful results than the other two approaches. As a result of these evaluations, it may be concluded that the suggested DMD and SST-based approaches that have lower computational complexity [28, 41] can successfully be used in the detection of epileptic EEG signals.

Acknowledgements

This paper was supported by Izmir Katip Celebi University Scientific Research Projects Coordination Unit: Project numbers: 2019-GAP-MÜMF-0003 and 2019-TDR-FEBE-0005.

Conflict of interest

The authors declare no conflicts of interest directly related to this study.

Thanks

We would like to thank Asst. Prof. Dr. Hatice Sabiha TÃ¼re and Asst.Prof.Dr. Sibel Kocaaslan Atli for their support in providing epileptic EEG recordings.

Abbreviations

EMD	empirical mode decomposition
EEMD	ensembe empirical mode decomposition
IMFs	intrinsic mode functions
DMD	dynamic mode decomposition
SST	synchrosqueezing transform
SC-DMD	single-channel DMD approach
MC-DMD	multi-channel DMD approach
DMD-HOS	higher-order DMD spectra
HOJ-TF	higher-order joint TF
GLCM	gray level co-occurrence matrix

Author details

Ozlem Karabiber Cura[1†] and Aydin Akan[2*†]

1 Department of Biomedical Engineering, Izmir Katip Celebi University, Cigli, Izmir, Turkey

2 Department of Electrical and Electronics Engineering, Izmir University of Economics, Balcova, Izmir, Turkey

*Address all correspondence to: akan.aydin@ieu.edu.tr

† These authors contributed equally.

References

[1] S Raghu, Natarajan Sriraam, Shyam Vasudeva Rao, Alangar Sathyaranjan Hegde, and Pieter L Kubben. Automated detection of epileptic seizures using successive decomposition index and support vector machine classifier in long-term eeg. *Neural Computing and Applications*, pages 1–20, 2019

[2] J. Song, Q. Li, B. Zhang, M. B. Westover, and R. Zhang. A new neural mass model driven method and its application in early epileptic seizure detection. *IEEE Transactions on Biomedical Engineering*, 67(8):2194–2205, 2020

[3] Manish Sharma, Ram Bilas Pachori, and U Rajendra Acharya. A new approach to characterize epileptic seizures using analytic time-frequency flexible wavelet transform and fractal dimension. *Pattern Recognition Letters*, 94:172–179, 2017

[4] Naghmeh Mahmoodian, Axel Boese, Michael Friebe, and Javad Haddadnia. Epileptic seizure detection using cross-bispectrum of electroencephalogram signal. *Seizure*, 66:4–11, 2019

[5] Qi Yuan, Weidong Zhou, Liren Zhang, Fan Zhang, Fangzhou Xu, Yan Leng, Dongmei Wei, and Meina Chen. Epileptic seizure detection based on imbalanced classification and wavelet packet transform. *Seizure*, 50:99–108, 2017

[6] OK Fasil and R Rajesh. Time-domain exponential energy for epileptic EEG signal classification. *Neuroscience Letters*, 694:1–8, 2019

[7] Emina Alickovic, Jasmin Kevric, and Abdulhamit Subasi. Performance evaluation of empirical mode decomposition, discrete wavelet transform, and wavelet packed decomposition for automated epileptic seizure detection and prediction. *Biomedical signal processing and control*, 39:94–102, 2018

[8] Ozlem Karabiber Cura, Sibel Kocaaslan Atli, Hatice Sabiha Türe, and Aydin Akan. Epileptic seizure classifications using empirical mode decomposition and its derivative. *BioMedical Engineering OnLine*, 19(1):1–22, 2020

[9] Zafer Iscan, Zümray Dokur, and Tamer Demiralp. Classification of electroencephalogram signals with combined time and frequency features. *Expert Systems with Applications*, 38(8): 10499–10505, 2011

[10] Jie Xiang, Conggai Li, Haifang Li, Rui Cao, Bin Wang, Xiaohong Han, and Junjie Chen. The detection of epileptic seizure signals based on fuzzy entropy. *Journal of neuroscience methods*, 243:18–25, 2015

[11] S Raghu, Natarajan Sriraam, Yasin Temel, Shyam Vasudeva Rao, Alangar Satyaranjandas Hegde, and Pieter L Kubben. Performance evaluation of dwt based sigmoid entropy in time and frequency domains for automated detection of epileptic seizures using svm classifier. *Computers in biology and medicine*, 110:127–143, 2019

[12] Qi Yuan, Weidong Zhou, Shufang Li, and Dongmei Cai. Epileptic EEG classification based on extreme learning machine and nonlinear features. *Epilepsy research*, 96(1-2):29–38, 2011

[13] Noha S Tawfik, Sherin M Youssef, and Mohamed Kholief. A hybrid automated detection of epileptic seizures in EEG records. *Computers & Electrical Engineering*, 53:177–190, 2016

[14] M Kemal Kıymık, İnan Güler, Alper Dizibüyük, and Mehmet Akın. Comparison of STFT and wavelet transform methods in determining

epileptic seizure activity in EEG signals for real-time application. *Computers in biology and medicine*, 35(7):603–616, 2005

[15] Barkın Büyükçakır, Furkan Elmaz, and Ali Yener Mutlu. Hilbert vibration decomposition-based epileptic seizure prediction with neural network. Computers in Biology and Medicine, 119:103665, 2020

[16] Susanta Kumar Rout and Pradyut Kumar Biswal. An efficient error-minimized random vector functional link network for epileptic seizure classification using VMD. *Biomedical Signal Processing and Control*, 57:101787, 2020

[17] Alexandros T Tzallas, Markos G Tsipouras, and Dimitrios I Fotiadis. Automatic seizure detection based on time-frequency analysis and artificial neural networks. *Computational Intelligence and Neuroscience*, 2007, 2007

[18] Kai Fu, Jianfeng Qu, Yi Chai, and Yong Dong. Classification of seizure based on the time-frequency image of EEG signals using HHT and SVM. *Biomedical Signal Processing and Control*, 13:15–22, 2014

[19] Ricardo Ramos-Aguilar, J. Arturo Olvera-López, Ivan Olmos-Pineda, and Susana Sánchez-Urrieta. Feature extraction from EEG spectrograms for epileptic seizure detection. *Pattern Recognition Letters*, 133:202–209, 2020

[20] Manish Sharma, Ram Bilas Pachori, and U. [Rajendra Acharya]. A new approach to characterize epileptic seizures using analytic time-frequency flexible wavelet transform and fractal dimension. *Pattern Recognition Letters*, 94:172–179, 2017

[21] M Deriche, S Arafat, S Al-Insaif, and M Siddiqui. Eigenspace time frequency based features for accurate seizure detection from EEG data. *IRBM*, 40(2): 122–132, 2019

[22] Shufang Li, Weidong Zhou, Qi Yuan, Shujuan Geng, and Dongmei Cai. Feature extraction and recognition of ictal EEG using EMD and SVM. *Computers in biology and medicine*, 43(7): 807–816, 2013

[23] Yang Zheng, Gang Wang, Kuo Li, Gang Bao, and Jue Wang. Epileptic seizure prediction using phase synchronization based on bivariate empirical mode decomposition. *Clinical Neurophysiology*, 125(6):1104–1111, 2014

[24] Asmat Zahra, Nadia Kanwal, Naveed ur Rehman, Shoaib Ehsan, and Klaus D. McDonald-Maier. Seizure detection from EEG signals using multivariate empirical mode decomposition. *Computers in Biology and Medicine*, 88:132–141, 2017

[25] Paschalis A Bizopoulos, Dimitrios G Tsalikakis, Alexandros T Tzallas, Dimitrios D Koutsouris, and Dimitrios I Fotiadis. EEG epileptic seizure detection using k-means clustering and marginal spectrum based on ensemble empirical mode decomposition. In *13th IEEE International Conference on BioInformatics and BioEngineering*, pages 1–4. IEEE, 2013

[26] S Ali, Mst Jannatul Ferdous, E Hamid, and KI Molla. Time-frequency coherence of multichannel EEG signals: Synchrosqueezing transform based analysis. *International Journal of Computer Science Trends and Technology*, 4(3):40–48, 2016

[27] Alireza Ahrabian, David Looney, Ljubiša Stanković, and Danilo P Mandic. Synchrosqueezing-based time-frequency analysis of multivariate data. *Signal Processing*, 106:331–341, 2015

[28] Shamzin Mamli and Hashem Kalbkhani. Gray-level co-occurrence matrix of fourier synchro-squeezed transform for epileptic seizure detection. *Biocybernetics and Biomedical Engineering*, 39(1):87–99, 2019

[29] Gaurav Thakur and Hau-Tieng Wu. Synchrosqueezing-based recovery of instantaneous frequency from nonuniform samples. *SIAM Journal on Mathematical Analysis*, 43(5):2078–2095, 2011

[30] Peter J Schmid. Dynamic mode decomposition of numerical and experimental data. *Journal of fluid mechanics*, 656:5–28, 2010

[31] Muhammad Sohaib J Solaija, Sajid Saleem, Khawar Khurshid, Syed Ali Hassan, and Awais Mehmood Kamboh. Dynamic mode decomposition based epileptic seizure detection from scalp EEG. *IEEE Access*, 6:38683–38692, 2018

[32] Muhammad Bilal, Muhammad Rizwan, Sajid Saleem, Muhammad Murtaza Khan, Mohammed Saeed Alkatheir, and Mohammed Alqarni. Automatic seizure detection using multi-resolution dynamic mode decomposition. *IEEE Access*, 7:61180–61194, 2019

[33] A Sharmila and P Geethanjali. DWT based detection of epileptic seizure from EEG signals using naïve bayes and k-NN classifiers. *Ieee Access*, 4:7716–7727, 2016

[34] Bingni W Brunton, Lise A Johnson, Jeffrey G Ojemann, and J Nathan Kutz. Extracting spatial–temporal coherent patterns in large-scale neural recordings using dynamic mode decomposition. *Journal of neuroscience methods*, 258:1–15, 2016

[35] Agustina Garcés Correa, Lorena Orosco, Pablo Diez, and Eric Laciar. Automatic detection of epileptic seizures in long-term EEG records. *Computers in biology and medicine*, 57:66–73, 2015

[36] Chuan Li and Ming Liang. A generalized synchrosqueezing transform for enhancing signal time–frequency representation. *Signal Processing*, 92(9):2264–2274, 2012

[37] Aydin Akan and R. Başar Ünsal. Time–frequency analysis and classification of temporomandibular joint sounds. *Journal of the Franklin Institute*, 337(4):437–451, 2000

[38] Mryka Hall-Beyer. GLCM texture: A tutorial. *National Council on Geographic Information and Analysis Remote Sensing Core Curriculum*, 3, 2000

[39] Kaveh Samiee, Serkan Kiranyaz, Moncef Gabbouj, and Tapio Saramäki. Long-term epileptic EEG classification via 2d mapping and textural features. *Expert Systems with Applications*, 42(20):7175–7185, 2015

[40] Siuly Siuly and Yan Li. Designing a robust feature extraction method based on optimum allocation and principal component analysis for epileptic eeg signal classification. *Computer Methods and Programs in Biomedicine*, 119(1):29–42, 2015

[41] N Benjamin Erichson, Steven L Brunton, and J Nathan Kutz. Compressed dynamic mode decomposition for background modeling. *Journal of Real-Time Image Processing*, 16(5):1479–1492, 2019